Eur. Phys. J. AP **5**, 209–214 (1999)

THE EUROPEAN PHYSICAL JOURNAL APPLIED PHYSICS

RDS and IRDS filters for fast CCD video sensors

N. Hassen[1], M. Jung[2], and B. Cunin[2,a]

[1] Faculté des Sciences, avenue de l'Environnement, 5000 Monastir, Tunisia
[2] Groupe d'Optique Appliquée, B.P. 28, 67037 Strasbourg Cedex 2, France

Received: 4 December 1997 /Revised: 7 July 1998 / Accepted: 30 October 1998

Abstract. In this paper we present two filters called Reflection Delayed noise Suppression RDS and Integration Reflection Delayed noise Suppression IRDS which are useful to increase the dynamics of video CCD cameras. The RDS is a band-pass filter built with a parallel short-circuited line. It lowers significantly the most important noise which is called reset noise. Unfortunately, this signal processing unit increases the contribution of thermal fluctuations by about 3 dB. To overcome this disadvantage, a triggered low-pass filter can be added to the RDS which leads to the IRDS cell. First, we will describe both systems, and then we will compare their effects, in a theoretical way and by experimentation, on the unsampled noises (*i.e.* the thermal and flicker noises) generated in the CCD sensor.

PACS. 83.85.Gk Sensors – 84.30.Bv Circuit theory (including computer-aided circuit design and analysis) – 84.30.Vn Filters

1 Introduction

The Correlated Double Sampling CDS is often used in order to decrease the noise introduced by resetting the floating diffusion sensing capacitance in the CCD readout register [1]. An other advantage of this technique is that it practically cancels the $1/f$ noise generated by the output amplifier, but it increases the thermal fluctuations by at least 3 dB.

The RDS circuit [2] theoretically gives the same results. Experimentally, it ensures a better attenuation of reset and $1/f$ noises [2] and its design is easier. An experimental study of a camera characterized by a pixel readout frequency of 8 MHz [3] demonstrated that this filter increases the sensitivity by about 7.5 dB. As it can run at frequencies greater than 20 MHz, it has been integrated in a numerical high speed camera operating at 1 000 frames per second [4].

In order to reduce this thermal noise accentuation, Nishida *et al.* [5] developed the "ICDS" filter by inserting, in both channels of the CDS, a low-pass circuit in which the capacitance was discharged before every pixel readout. We used the same principle for the RDS system by adding a triggered low-pass filter which integrates the signal and the remaining noise during the 2/5 of the pixel period T_e. This system called "IRDS" is equivalent to the ICDS circuit, but its simple structure allows it be used in high speed video cameras.

[a] e-mail: cunin@goa.c-strasbourg.fr

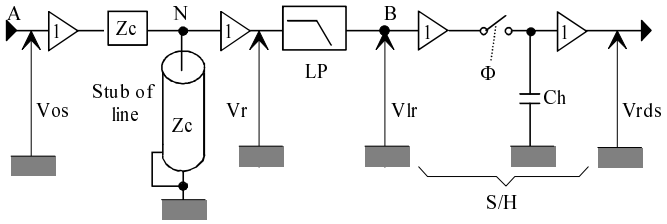

Fig. 1. Simplified drawing of the RDS filter.

2 Description of the noise reduction circuits RDS and IRDS

2.1 RDS filter

The RDS filter uses a parallel short-circuited stub of characteristic impedance Z_c which is inserted between two buffers with low output and high input impedance (Fig. 1). Since the input of this line is adapted, the voltage $V_r(t)$ measured at node N is the difference between the incident wave $V_{os}(t)/2$ and the reflected voltage $V_{os}(t-2\tau_r)/2$ where τ_r represents the propagation time in the line. The circuit is completed by a low-pass filter (LP) with a cut-off pulsation ω_0 and by a zero order sample and hold (S/H). The purpose of the LP filter is to reduce the spectral aliasing of the thermal noise due to the sampling.

We will suppose (Fig. 2) that the video signal starts at $t = 0$ and that the readout capacitance of the sensor is reset from $\tau = 0.4T_e$ to $0.6T_e$. In this case, the duration of the floating level is also equal to $0.4T_e$. If we choose $2\tau_r \cong 0.4T_e$, the voltage V_r in the time interval $[0–\tau]$, is the difference between the pixel peak level and its floating

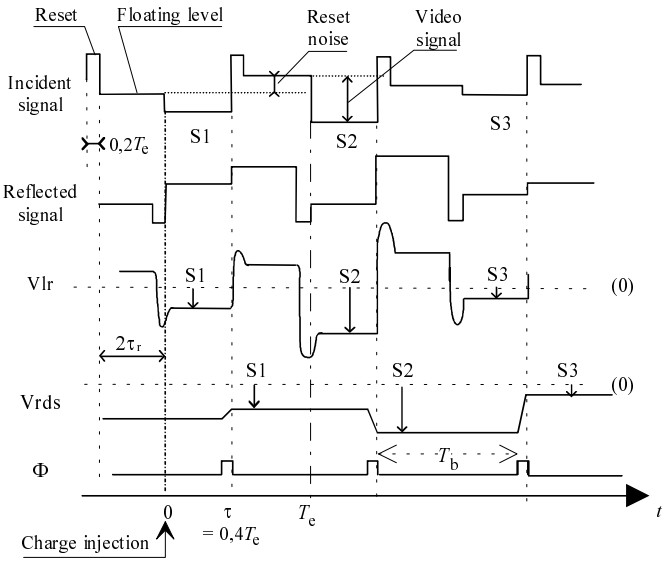

Fig. 2. RDS filter signals.

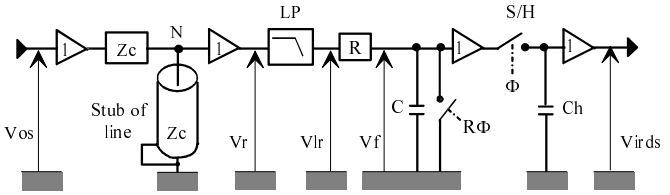

Fig. 3. Functional drawing of the IRDS filter.

level. This subtraction highly attenuates the reset noise. At time τ when the clock Φ is going high, the video signal is sampled and held during the time T_b.

If the delay line losses are negligible, V_r can be written as:

$$V_r(t) = \frac{1}{2}\left[V_{os}(t) - V_{os}(t - 2\tau_r)\right] \tag{1}$$

and for a first order low-pass filter the frequency transfer function between A and B is:

$$H_{rds}(\omega) = \frac{j\sin(\omega\tau_r)}{[1 + j\omega/\omega_0]}\exp(-j\omega\tau_r). \tag{2}$$

It is important to note that this filter does not include any switch other than the S/H switch which, in numerical cameras, is integrated on the ADC. This simple design guarantees that the RDS can run at high frequencies ($>$ 20 MHz). Moreover, the chosen configuration with a parallel short-circuited line is a very simple way to delay a half of the video signal and to perform the subtraction (1) involved in the reset noise rejection.

2.2 IRDS filter

It is built with a RDS filter followed by a triggered low-pass circuit (Fig. 3) with a time constant of charge RC ($> 2T_e$). The principle of operation is illustrated by Figure 4.

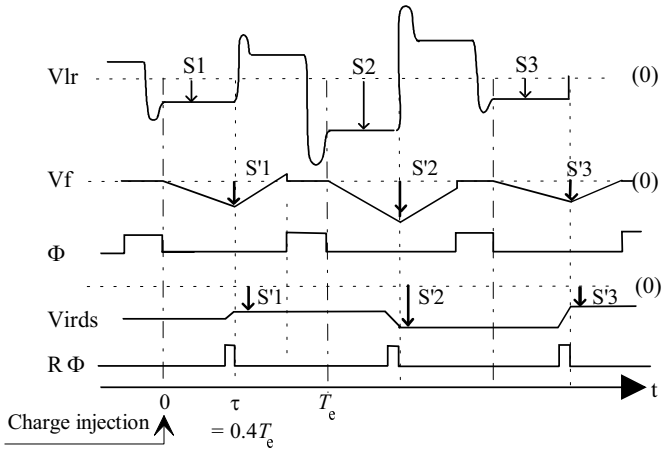

Fig. 4. IRDS filter signals.

At the beginning of each pixel readout, the switch triggered by the $R\Phi$ clock is closed. It is opened when the charge is injected in the conversion capacitance and the voltage V_{lr} is integrated by the RC circuit from 0 to $\tau\,(\cong 0.4T_e)$ at which it is sampled and held. The capacitance C is then short-circuited when the clock $R\Phi$ is high.

A straightforward analysis shows that this circuit (without S/H) is characterized by the frequency transfer function:

$$\begin{aligned} H_{irds} &= \left[\frac{1 - \exp(-\tau/RC)\exp(-j\omega\tau)}{1 + jRC\omega}\right] \\ &\quad \times \frac{j\sin(\omega\tau_r)}{[1 + j\omega/\omega_0]}\exp(-j\omega\tau_r) \\ &\cong \frac{1 - (1 - \tau/RC)\exp(-j\omega\tau)}{[1 + jRC\omega]\,[1 + j\omega/\omega_0]} \\ &\quad \times j\sin(\omega\tau_r)\exp(-j\omega\tau_r) \qquad \text{if } RC \geq 5\tau. \end{aligned} \tag{3}$$

3 Unsampled noise filtering

We now have to compare theoretically the filtering characteristics of the RDS or IRDS for the thermal and $1/f$ noises generated by the readout stage of the CCD sensor.

It is important to recall that the spectral aliasing is limited by the low-pass filter for the RDS, by the triggered integrating cell for the IRDS, and to note that the random processes considered are stationary and completely uncorrelated between two consecutive resets. In these conditions, we can assume that the ratio of the spectral density after the RDS to the spectral density after the IRDS remains roughly the same with or without the S/H. This approximation greatly simplifies the calculations but it clearly fails for the reset noise which is uncorrelated only from pixel to pixel.

The power spectral density of the unsampled noise can be written as:

$$S_e(\omega) = 4R_nKT\left[1 + \left(\frac{2\pi f_t}{\omega}\right)^{\alpha}\right] \tag{4}$$

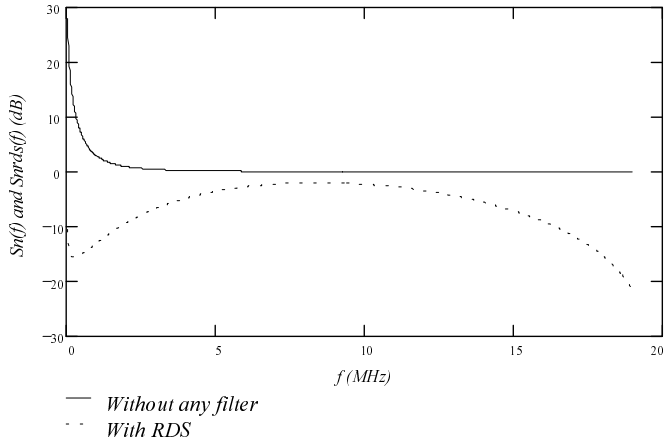

Fig. 5. Theoretical spectral distribution of the unsampled noise without and with the RDS.

where K is the Boltzmann constant, T the absolute temperature, R_n (< 10 kΩ) the thermal noise equivalent resistance, f_t (≤ 1 MHz) the transition frequency and α a constant parameter such as: $1 \leq \alpha \leq 2$. We will take $\alpha = 2$ in order to simplify the evaluation of forthcoming integrals.

3.1 RDS circuit

Taking (2) into account, the power spectral density of the unsampled noise before the S/H circuit is given by:

$$S_{rds}(\omega) = S_e(\omega)\frac{\omega_0^2 \sin^2(\omega\tau_r)}{\omega^2 + \omega_0^2} \cdot \tag{5}$$

To clearly describe the filtering of the RDS, we plot hereafter the normalized functions $S_n(\omega)$ $(= S_e(\omega)/4R_nKT)$ and $S_{nrds}(\omega)\,(= S_{rds}(\omega)/4R_nKT)$ for $f_t = 1$ MHz, $f_e = 8$ MHz, $\tau_r = 25$ ns and $f_0 = 12$ MHz.

These curves show that the RDS practically cancels the flicker noise and that it only introduces a minimal attenuation of about 2 dB at the readout frequency (8 MHz). This circuit is a pass-band filter with a large 3 dB bandwidth (~ 8 MHz) which guarantees a good transmission of the CCD signal. Such a circuit built with lumped elements would require an inductance of about 1 μF which is rather cumbersome. As we need a stub of line to delay the video signal, it is more advantageous to use this line as a distributed resonator. However, this solution presents the drawback of multiple resonances which are attenuated by the low-pass filter.

More precisely the thermal noise variance at the RDS filter output is:

$$\begin{aligned}\sigma_{th}^2\big|_{RDS} &= \frac{4R_nKT}{2\pi}\int_0^\infty \frac{\omega_0^2 \sin^2(\omega\tau_r)}{\omega^2+\omega_0^2}d\omega \\ &= \frac{R_nKT\omega_0}{2}\left[1-\exp(-\omega_0 2\tau_r)\right]\cdot\end{aligned} \tag{6}$$

In the same way, we found for the $1/f^2$ noise:

$$\sigma_{1/f^2}^2\big|_{RDS} = 2\pi^2 R_nKTf_t^2\left[2\tau_r - \frac{1}{\omega_0}\left[1-\exp(-\omega_0 2\tau_r)\right]\right]\cdot \tag{7}$$

In order to reduce the cross talking between consecutive pixels, the cut-off frequency f_0 of the low pass filter must be at least equal to the readout frequency f_e. In this condition and recalling that: $2\tau_r \cong 0.4T_e$, it is easy to show that:

$$\left.\frac{\sigma_{1/f^2}^2}{\sigma_{th}^2}\right|_{RDS} \approx \left(\frac{f_t}{f_0}\right)^2(2\tau_r\omega_0 - 1) < \left(\frac{f_t}{f_e}\right)^2\cdot \tag{8}$$

Usually, the transition frequency f_t (≤ 1 MHz) is much lower than the readout frequency f_e. We conclude that the contribution of the $1/f^2$ noise is negligible and that the total noise variance is given by:

$$\sigma_{ne}^2\big|_{RDS} \approx \sigma_{th}^2\big|_{RDS} = \frac{R_nKT\omega_0}{2}\left[1-\exp(-\omega_0 2\tau_r)\right]\cdot \tag{9}$$

By neglecting the transients of the reset state and by assimilating the video signal to a rectangular pulse with an amplitude E_i, the output voltage measured at the sampling time τ is:

$$V_{RDS} = \frac{E_i}{2}\left[1-\exp(-\omega_0\tau)\right]\cdot \tag{10}$$

With $\tau = 2\tau_r = 0.4T_e$ the signal to unsampled noise ratio is given by:

$$\left.\left(\frac{S}{N}\right)_{ne}\right|_{RDS} = \frac{E_i}{\sqrt{2R_nKT}}\frac{\left[1-\exp(-\omega_0\tau_r)\right]}{\sqrt{\omega_0\left[1-\exp(-2\omega_0\tau_r)\right]}}\cdot \tag{11}$$

This expression shows that this ratio increases when the cut-off frequency ω_0 of the low-pass filter decreases. However, a too low ω_0 value reduces the spatial resolution of the camera and the reset noise attenuation [6]. In the following part, we will take: $f_0 \cong 1.5f_e$. This choice corresponds to an overall cut-off frequency near f_e and it is a good compromise between the signal-to-noise ratio and the spatial resolution of the camera. In these conditions, we can write:

$$\left.\left(\frac{S}{N}\right)_{ne}\right|_{RDS} \approx 0.227\frac{E_i}{\sqrt{R_nKT}}\sqrt{T_e}\cdot \tag{12}$$

It is interesting to compare this result to the one obtained without the RDS cell. By assuming that the cut-off frequency of the anti-aliasing low-pass filter is equal to the overall bandwidth above ($f_0 \cong f_e$) and by considering only the thermal noise, we have:

$$\left.\left(\frac{S}{N}\right)_{th}\right|_{Cla} = \frac{E_i\left[1-\exp(-\omega_e\tau)\right]}{\sqrt{R_nKT}\sqrt{\omega_e}} \approx 0.366\frac{E_i}{\sqrt{R_nKT}}\sqrt{T_e}\cdot \tag{13}$$

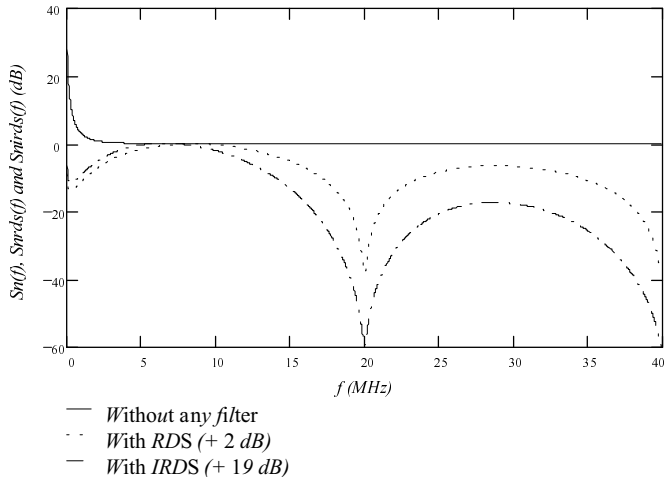

Fig. 6. Theoretical spectral distribution of the unsampled noise without and with the RDS or the IRDS.

We conclude that the RDS circuit reduces this signal to noise ratio by about 4 dB (3 dB for the same low-pass filter cut-off frequency, *i.e.* $f_0 \cong 1.5 f_e$). However, it makes negligible the $1/f^a$ noise which is visually very uncomfortable.

3.2 IRDS circuit

Taking (3) into account, the unsampled noise variance at the IRDS filter output is:

$$\sigma_{ne}^2\big|_{IRDS} = \frac{1}{2\pi}\int_0^\infty S_e(\omega)\,|H_{irds}(\omega)|^2\,d\omega \qquad (14)$$

with

$$|H_{irds}(\omega)|^2 = \frac{1-2\exp(-\tau/RC)\cos\omega\tau+\exp(-2\tau/RC)}{\left[1+(RC\omega)^2\right]\left[1+(\omega/\omega_0)^2\right]} \times \sin^2(\omega\tau_r) \cong \left(1-\frac{\tau}{RC}\right)\frac{4\sin^2(\omega\tau/2)\sin^2(\omega\tau_r)}{\left[1+(RC\omega)^2\right]\left[1+(\omega/\omega_0)^2\right]} \quad \text{for } RC \geq 5\tau. \qquad (15)$$

As for the RDS filter we define the normalized power spectral density at the output of the IRDS cell (without S/H):

$$S_{nirds}(\omega) = S_n(\omega)\,|H_{irds}(\omega)|^2\,. \qquad (16)$$

The functions $S_n(\omega)$, $S_{nrds}(\omega)$ and $S_{nirds}(\omega)$ are plotted in Figure 6 for $f_t = 1$ MHz, $f_e = 8$ MHz, $f_0 = 12$ MHz, $\tau = 2\tau_r = 50$ ns and $RC = 5\tau = 250$ ns.

We have added respectively 2 and 19 dB to the values of S_{nrds} and of S_{nirds} in order to compensate the transmission loss of the RDS or of the IRDS at frequencies near f_e. Thanks to that transformation, it is evident that the rejection of the $1/f^2$ noise is almost the same for both filters and that above 10 MHz the thermal noise is more attenuated by the IRDS than by the RDS. Consequently, we conclude that the signal to noise ratio of the IRDS is higher than that of the RDS and that the spectral aliasing due to the sampling is highly reduced for the IRDS.

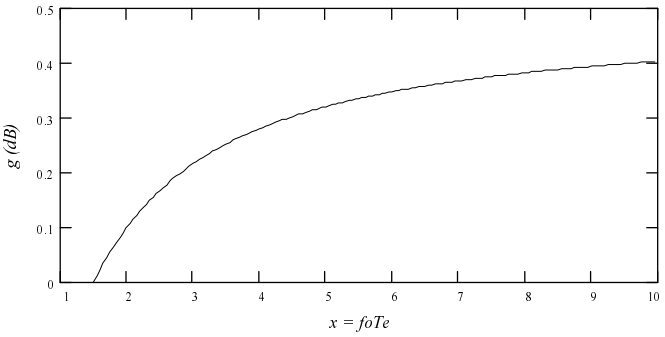

Fig. 7. S/N ratio *versus* f_0.

Remarking that we have:

$$|H_{irds}(\omega)|^2 \approx \left(1-\frac{\tau}{RC}\right)\omega^4\tau^2\tau_r^2 \approx 0 \quad \text{for } \omega < \frac{1}{RC} \leq \frac{0.2}{\tau} = \frac{0.1}{\tau_r} \qquad (17)$$

we only make a small error in (13) if we write:

$$\sigma_{ne}^2\big|_{IRDS} = \left(1-\frac{\tau}{RC}\right)\frac{2}{\pi(RC)^2} \times \int_0^\infty S_e(\omega)\frac{\sin^2(\omega\tau/2)\sin^2(\omega\tau_r)}{\omega^2\left[1+(\omega/\omega_0)^2\right]}d\omega. \qquad (18)$$

By proceeding as before, we obtain after the IRDS:

$$\sigma_{th}^2\big|_{IRDS} \cong \left(1-\frac{\tau}{RC}\right)\frac{R_nKT}{(RC)^2} \times \left[\tau-\frac{1}{\omega_0}\{1-\exp(-\tau\omega_0)+\exp(-2\tau_r\omega_0) \times [\cosh(\tau\omega_0)-1]\}\right] \quad \text{with } \tau \leq 2\tau_r \qquad (19)$$

$$\sigma_{1/f^2}\big|_{IRDS} \cong \left(1-\frac{\tau}{RC}\right)\frac{4\pi^2R_nKTf_t^2}{(RC)^2} \times \left[\frac{1}{\omega_0^3}\{1-\exp(-\tau\omega_0)+\exp(-\omega_0 2\tau_r) \times [\cosh(\omega_0\tau)-1]\}-\frac{\tau}{\omega_0^2}+\frac{\tau^2}{6}(6\tau_r-\tau)\right] \quad \text{if } \tau \leq 2\tau_r. \qquad (20)$$

As for the RDS, it is not difficult to show that, for $f_0 \geq 1.5 f_e$, the $1/f^2$ noise is negligible comparatively to the thermal noise and the unsampled noise variance is practically given by (19).

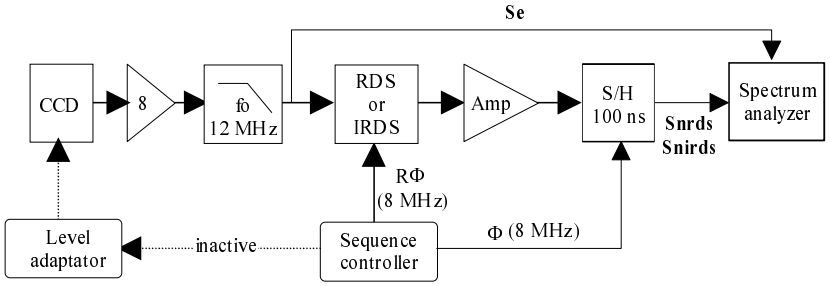

Fig. 8. Functional drawing of the measure circuit.

Recalling that the integration time is such that $\tau \ll RC$, the sampled video signal amplitude is:

$$V_{IRDS} \cong \frac{E_i}{2RC} \int_0^{\tau} [1 - \exp(-\omega_0 t)]\, dt = \frac{E_i \tau}{2RC} \left[1 + \frac{\exp(-\omega_0 \tau) - 1}{\omega_0 \tau}\right]. \quad (21)$$

If we put $x = f_0/f_e$ and take $\tau = 2\tau_r$, the signal to noise ratio can be written as:

$$\left(\frac{S}{N}\right)_{ne}\Bigg|_{IRDS} \cong \frac{E_i\sqrt{\tau}}{2\sqrt{R_n K T}} \left(1 + \frac{\tau}{2RC}\right) y(x) \quad (22)$$

where

$$y(x) = \frac{\left[1 + \frac{\exp(-x\omega_e\tau)-1}{x\omega_e\tau}\right]}{\sqrt{1 - \frac{1}{x\omega_e\tau}\left\{1 + \exp(-x\omega_e\tau)\left[\mathrm{ch}(x\omega_e\tau) - 2\right]\right\}}} \cdot \quad (23)$$

The S/N ratio does not depend very much on the time constant RC and, for $x = 1.5$, $RC = 5\tau = 2T_e$, it is equal to:

$$\left(\frac{S}{N}\right)_{ne}\Bigg|_{IRDS} \approx 0.329 \frac{E_i}{\sqrt{R_n K T}} \sqrt{T_e} \cdot \quad (24)$$

According to the relation (12), this result shows that the IRDS circuit improves the signal to unsampled noise ratio of about 3.2 dB comparatively to the RDS filter.

3.3 Optimization of IRDS filter S/N ratio

The variation of the S/N ratio with the cut-off frequency f_0 is determined by the function $y(x)$ defined above. It is best represented by the logarithmic normalized function $g(x)$:

$$g(x) = 20 \log \left[\frac{y(x)}{y(1.5)}\right] \quad (25)$$

which is shown in Figure 7 for $\tau = 2\tau_r = 0.4T_e$.

It demonstrates that the signal to unsampled noise ratio slightly increases with f_0. In practice, this parameter is limited by the bandwidth of the output CCD stage ($\sim$ 90 MHz for sensors used in high speed video) and by that of the amplifiers associated with the IRDS. Taking account of the transmission loss of the IRDS and of the level matching between the CCD output and the ADC input, we need an amplification of approximately 36 dB. In this case and by using current feedback amplifiers, the overall bandwidth is estimated to 50 MHz which corresponds to $x \sim 6$ for $f_e = 8$ MHz. Therefore we conclude that the IRDS filter improves the S/N ratio by about 3.5 dB comparing to the RDS circuit.

4 Experimental study

4.1 Setup

This study has been achieved on a camera built with the frame transfer sensor EEV-CCD 17 (512 × 512 pixels). This sensor contains two output registers running at a frequency f_e of 8 MHz [3]. By holding all sensor phases constant, only the unsampled noise generated by the readout stage is transferred to the measure chain.

Figure 6 shows a simplified diagram of the experimental setup. A spectral analyzer (HP 8591E) is used to measure the noise spectral density between 9 kHz and 12 MHz with a preamplifier gain close to 8 and a cut-off frequency f_0 of 12 MHz. This study has been repeated with and without the RDS and IRDS. In each case, the gain of the amplifier "Amp" has been adjusted in order to keep the same video level before sampling (Fig. 8).

4.2 Experimental results

The spectral distributions of noises filtered by the RDS or the IRDS have been measured after the S/H with a hold time T_b of 100 ns. On the contrary, we have determined the power spectral density S_e without the S/H. The purpose of this choice is to avoid aliasing in order to simplify the determination of the noise resistance R_n and of the transition frequency f_t.

Figure 9 summarizes the experimental data. Without filtering, the $1/f$ noise is greater than the thermal contribution for frequencies less than $f_t \approx 1$ MHz. Taking into

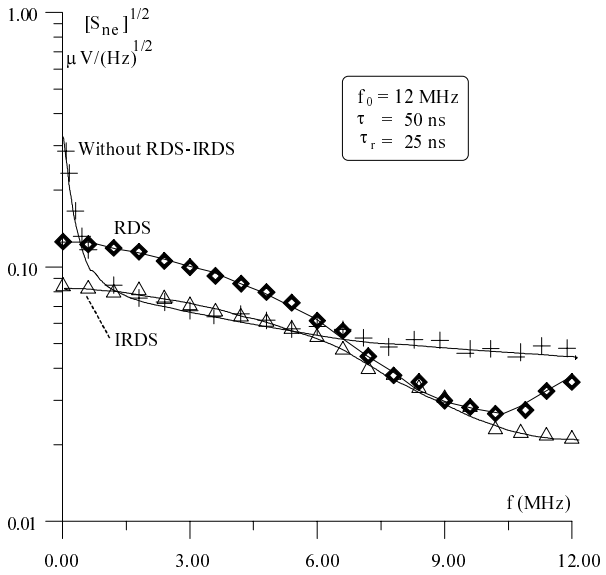

Fig. 9. Spectral distribution of the unsampled noise.

account the preamplifier gain (18 dB) and the attenuation due to the low-pass filter, the spectral density of the Johnson noise at the CCD output is near to 8×10^{-17} V^2/Hz, which is equivalent to a noise resistance R_n close to 5 kΩ.

As expected, both filters eliminate almost the $1/f$ noise, but the RDS increases the thermal fluctuations by about 3 dB, whereas the IRDS corrects practically this effect.

Except for the frequency near to 10 MHz, the measured distribution curves of the noise filtered by the RDS or by the IRDS are in good agreement with numerical simulations that we have performed taking into account the spectral aliasing due to the S/H circuit. Theoretically, there should be a notch with an infinite attenuation at 10 MHz ($= 1/T_b$). In fact, this rejection is limited by the noise floor of the spectrum analyzer ($\sim 4 \times 10^{-16}$ V^2/Hz). There is also a small problem, for which we do not have any explanation, in the way the IRDS works in the band 10–12 MHz. Nevertheless, it appears that the RDS and IRDS models developed above are quite good. Consequently, we can conclude, in accordance with the analysis developed above, that the S/N ratio of the IRDS filter is higher by about 3 dB than that of the RDS circuit. This conclusion is approximately valid for the continuous signal at the output of the filters and for the signal delivered by the S/H circuit.

5 Conclusion

The IRDS filter corrects in a major part the RDS increasing of thermal noise which is of 3 to 4 dB comparing to a direct output. This improvement of the S/N ratio is reached for a preamplifier bandwidth as wide as possible. Both circuits highly attenuate the $1/f$ noise.

Thanks to their simple structure, they can run up to frequencies greater than 20 MHz. Hence, they can be integrated in high speed video cameras which usually use CCD sensor with a readout frequency near 20 MHz. However, in this case the duration of the floating state (20 ns) is too short and the floating level cannot reach the reset voltage before the charges are injected into the conversion capacitance. Therefore the RDS filter will increase the reset noise by 3 dB. This undesirable effect can be almost corrected by using an IRDS signal processing circuit.

References

1. W.H. White *et al.*, IEEE J. Sol. Stat. Circ. **SC 9**, 1 (1974).
2. M. Ohbo *et al.*, IEEE Trans. Cons. Electron. **35** (1989).
3. N. Hassen, Ph.D. thesis, University Louis-Pasteur, Strasbourg, 1995.
4. M. Jung *et al.*, QCAV'97 International Conference on Quality Control by Artificial Vision, Le Creusot, France, (1997).
5. Y. Nishida *et al.*, IEEE Trans. Electron Dev. **36** (1989).
6. J. Hynecek, in IEEE Trans. Electron Dev. **37**, 3 (1992).